arXiv:1608.05218v2 [hep-ph] 29 Nov 2016

Small size sources of secondaries observed in pp-collisions via Bose-Einstein correlations at the LHC ATLAS experiment

V.A. Schegelsky and M.G. Ryskin

Petersburg Nuclear Physics Institute, NRC 'Kurchatov Institute', Gatchina, St. Petersburg, 188300, Russia

Abstract

Bose-Einstein correlations in proton-proton collisions at the LHC are well descried by the formula with two different scales. It is shown for the first time that the pions are produced by few small size sources distributed over a much larger area in impact parameter space occupied by the interaction amplitude. The dependence of the two radii obtained in this procedure on the charged particle density and the mean transverse momentum of the pion/hadron in the correlated pair are discussed.

1 Introduction

An effective tool to study the space-time structure of the production amplitude is to measure the Bose-Einstein correlations (BEC) between two identical particles produced in the inclusive hadron interaction, see, for example, [1]– [4]. The idea is as follows. To satisfy the Bose-Einstein statistics we have to sum up the amplitudes with all the permutations of the identical secondary bosons. After the permutation of two bosons (pions) the amplitude gets the factor $\exp(irq)$, where 4-vectors $q = p_2 - p_1$ is the difference between the pions momenta while $r = r_1 - r_2$ is the space separation between these pions. So the two particle cross section corresponding to the bare production amplitude $M(....r_1, r_2, ...)$ becomes

$$\frac{E_1 E_2 d^2\sigma}{d^3p_1 d^3p_2} \;=\; \frac{1}{2!}|M|^2\langle 2+2e^{irq}\rangle \;=\; |M|^2\,\langle 1+e^{irq}\rangle \tag{1}$$

proportional to the the factor $(1+ < \exp(irq) >)$. The $\langle ...\rangle$ denote the averaging over r_1 and r_2. Due to fast oscillations, for a large q the mean value of this exponent vanishes after the integration over the $r_{1,2}$-coordinates. On the other hand $< \exp(irq) > \to 1$ for a very low q, enlarging the cross section two times. So we have a peak at $q \to 0$ and the inverse width of the peak characterizes the size of the domain from which the pions were emitted.

To extract the effect the measured Q spectrum

$$Q = \sqrt{-(p_1 - p_2)^2}. \tag{2}$$

is compared with a similar one but without BEC. Q is the invariant mass of two BEC particles considered as massless. To be precise we form the ratio

$$R(Q) \;=\; \frac{dN/dQ \;-\; dN_{\rm ref}/dQ}{dN_{\rm ref}/dQ} \tag{3}$$

where dN/dQ is the two pion distribution integrated over all the variables except Q , and $dN_{\rm ref}/dQ$ is the distribution expected in a world without BEC. There are different ways to choose $dN_{\rm ref}/dQ$. We may measure the $\pi^+\pi^-$ distribution for non-identical pions; or we may change the sign of the three momentum of the second pion $\vec{p}_2 \to -\vec{p}_2$; and so on. For the conventional 'one-radius' fit the simplest parametrization is usually used:

$$R(Q) = \lambda e^{-RQ} + a + bQ. \tag{4}$$

Parameter R = $\bar{r}$ is the radius of the radiation area [1] , λ can be called as a strength of BEC, and a and b describe a simplest background to BEC. The exponential form approximates the case when radiation sources are uniformly distributed over the surface of the sphere with radius $\bar{r}$. The values of R are extracted from the data, using one or another reasonable reference function $dN_{\rm ref}/dQ$, are close to each other. Such analysis of high energy proton-proton interactions at the LHC have been performed by ATLAS [5], CMS [6] and ALICE [7]. For an analysis of lower energy data see, for example, the review in Ref. [4]

However it was argue in [8] that the distribution of the coordinates of emission requires two scales and secondaries produced in high energy hadron collisions may be radiated by *small size* sources distributed over a much larger area of the proton-proton interaction. To study this point experimentally we re-analyze the existing ATLAS data on BEC at $\sqrt{s} = 0.9$ and 7 TeV fitting the $R(Q)$ distribution by the formula with two scales

$$R(Q) \;=\; \lambda \; e^{-R1Q} + (1-\lambda)\; e^{-R2Q} \tag{5}$$

Note that we do not introduce two parameters, λ_1 and λ_2 but in agreement with (1) fix the sum $\lambda_1 + \lambda_2 = 1$; i.e. $\lambda_1 = \lambda$ and $\lambda_2 = 1 - \lambda$. ***In such approach R2 is the radius of radiation source BUT R1 is the distance between two sources i.e. full size of the radiation zone with a maximum value equal to proton radius*** R_p***!***

The ATLAS experiment set up and event selection are described in [5]. Here we just emphasize that it is a huge statistics available in the LHC experiments (about 10^7 minimum bias events in the

[1] The 'mean' radius, $\bar{r}$, is such that $e^{-\bar{r}Q}$ approximates the value of e^{irq} averaged over r .

case of ATLAS at 7 TeV corresponding to more than 10^9 pairs of same sign secondary hadrons) which allow to reanalyze data with the *two* scales[2] and to study not just the size of the radiative domain but the structure of the hadron production process. In sect.2 we present the results of the new analysis and in sect.3 we discuss the possible interpretation of the main features observed. We conclude in sect.4.

2 Two scales analysis

The 'reference' distribution dN_{ref}/dQ was obtained by changing the sign of three momentum of the second hadron $\vec{p}_2 \to -\vec{p}_2$ [3]. In our re-analysis of the minimum bias data obtained by ATLAS at 0.9 and 7 TeV were used. For the details of the experiment and events selection see [5]. Here we consider all charged hadrons as pions and select the particles with transverse momentum $p_t > 0.1$ GeV in the pseudorapidity interval $|\eta| < 2.5$ observed in the central detector. The majority of these hadrons are the pions.

The description of the data is shown in Fig.1.

The quality of the fit with two different radii is quite good. The value of χ^2 turns out to be more than order of magnitude less than that in conventional *one* scale fit (4). At 7 TeV we get $\chi^2/dof = 1.6$ describing *all* the selected same sign pairs. Recall that the value of mean radius, R, depends on the particle density, $dN_{ch}/d\eta$ [4] , in a particular event. This effect was observed first time [9] by UA1 collaboration in 1989. Therefore we can not expect too small χ^2 if the statistics is high. Of course, fitting the data in an adequate small bins of the final state phase space to make statistics in fits smaller, one can get $\chi^2/dof.$ close to one.

The qualitative features of the distributions at 900 GeV are very similar to that at 7 TeV but the statistics at 7 TeV is much higher. Therefore below we will present the results for 7 TeV only. The dependencies of the mean radii and the correlation strength, $\lambda_{1,2}$ on particles multiplicity N_{ch} are shown in Fig.2.

Finally in Fig.3 we show the dependence of both radii on the mean transverse momentum $k_t = (p_1 + p_2)_t/2$ of the hadrons in a pair. Here all N_{ch} bins are included into the fit.

3 Discussion

Following the original paper [8], where it was proposed to introduce two scales description of BEC, we will focus on the interpretation of obtained result in terms of a multi-Pomeron approach. Here

[2] details will be published elsewhere

[3] this the only difference with [5] in determination (3). Note that in comparison with [5] we did not use in (3) the double ration. It is not needed to fit the data.

[4] $dN_{ch}/d\eta$ should be used if experiments have different η acceptance; ATLAS and CMS LHC experiments have nearly identical η acceptance and multiplicity distribution N_{ch} may be used.

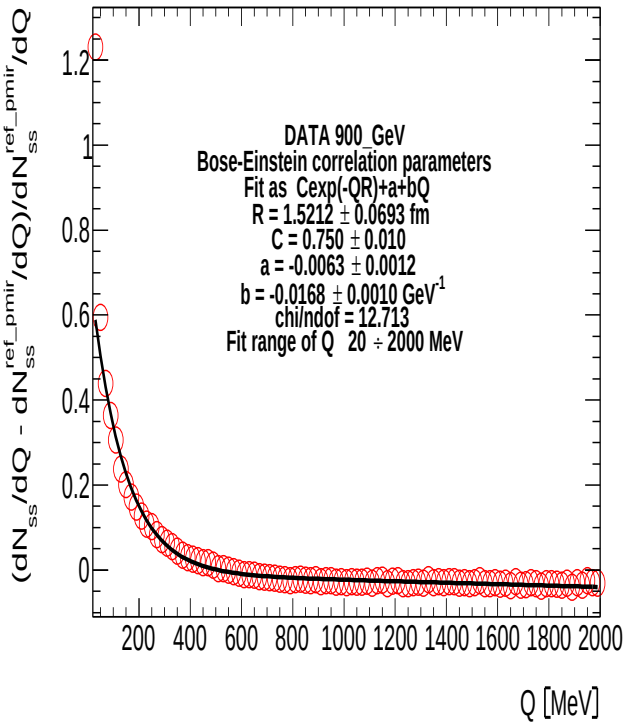
DATA 900_GeV
Bose-Einstein correlation parameters
Fit as Cexp(-QR)+a+bQ
R = 1.5212 ± 0.0693 fm
C = 0.750 ± 0.010
a = -0.0063 ± 0.0012
b = -0.0168 ± 0.0010 GeV-1
chi/ndof = 12.713
Fit range of Q 20 ÷ 2000 MeV
(dNss/dQ - dNssref_pmir/dQ)/dNssref_pmir/dQ
Q [MeV]

(a) 900 GeV data dR/dQ distribution with one radius structure function

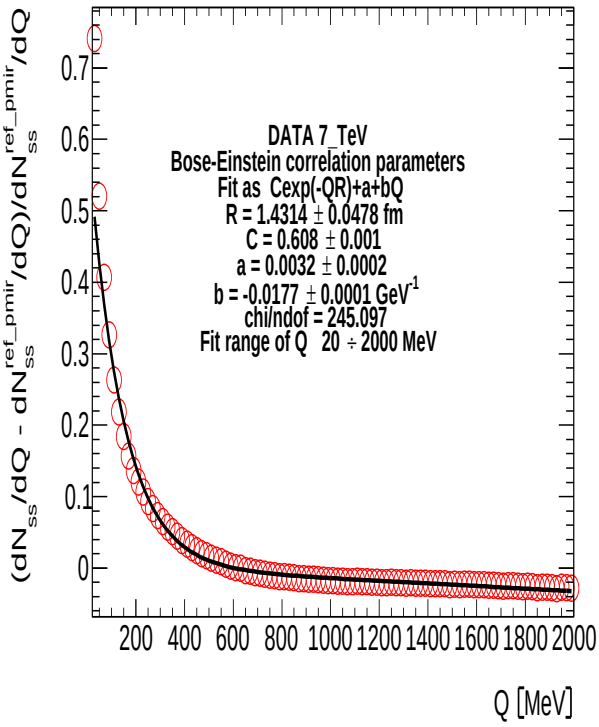
DATA 7_TeV
Bose-Einstein correlation parameters
Fit as Cexp(-QR)+a+bQ
R = 1.4314 ± 0.0478 fm
C = 0.608 ± 0.001
a = 0.0032 ± 0.0002
b = -0.0177 ± 0.0001 GeV-1
chi/ndof = 245.097
Fit range of Q 20 ÷ 2000 MeV
(dNss/dQ - dNssref_pmir/dQ)/dNssref_pmir/dQ
Q [MeV]

(b) 7TeV data dR/dQ distribution with one radius structure function

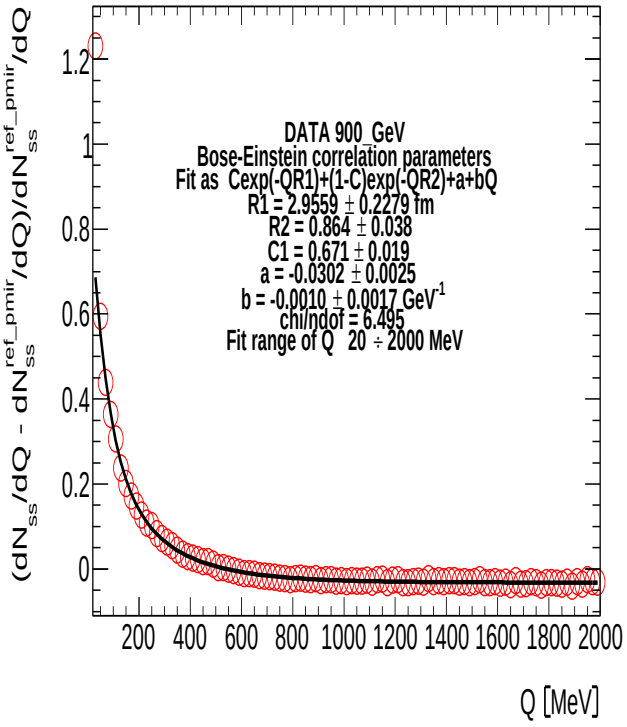
DATA 900_GeV
Bose-Einstein correlation parameters
Fit as Cexp(-QR1)+(1-C)exp(-QR2)+a+bQ
R1 = 2.9559 ± 0.2279 fm
R2 = 0.864 ± 0.038
C1 = 0.671 ± 0.019
a = -0.0302 ± 0.0025
b = -0.0010 ± 0.0017 GeV-1
chi/ndof = 6.495
Fit range of Q 20 ÷ 2000 MeV
(dNss/dQ - dNssref_pmir/dQ)/dNssref_pmir/dQ
Q [MeV]

(c) 900 GeV data dR/dQ distribution with two radii structure functions

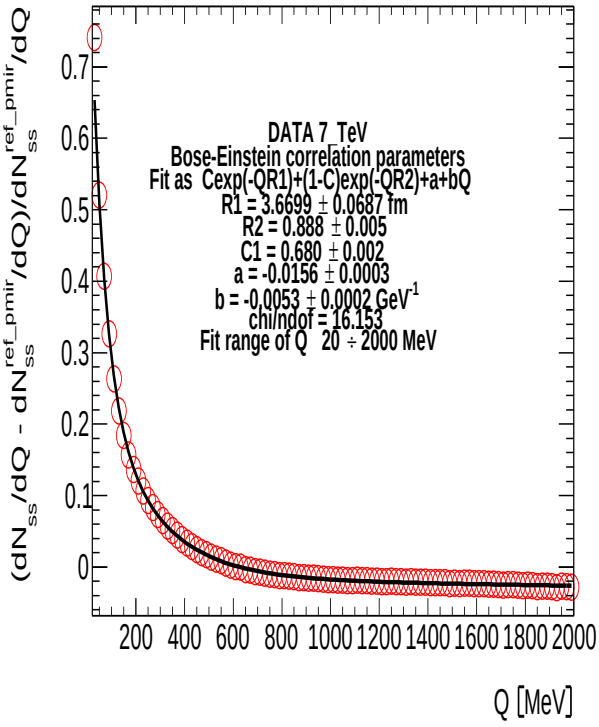
DATA 7_TeV
Bose-Einstein correlation parameters
Fit as Cexp(-QR1)+(1-C)exp(-QR2)+a+bQ
R1 = 3.6699 ± 0.0687 fm
R2 = 0.888 ± 0.005
C1 = 0.680 ± 0.002
a = -0.0156 ± 0.0003
b = -0.0053 ± 0.0002 GeV-1
chi/ndof = 16.153
Fit range of Q 20 ÷ 2000 MeV
(dNss/dQ - dNssref_pmir/dQ)/dNssref_pmir/dQ
Q [MeV]

(d) 7TeV data dR/dQ distribution with two radii structure function

Figure 1: One and two radii global fit of dR/dQ distributions at $\sqrt{s}$= 900 GeV and 7 TeV.

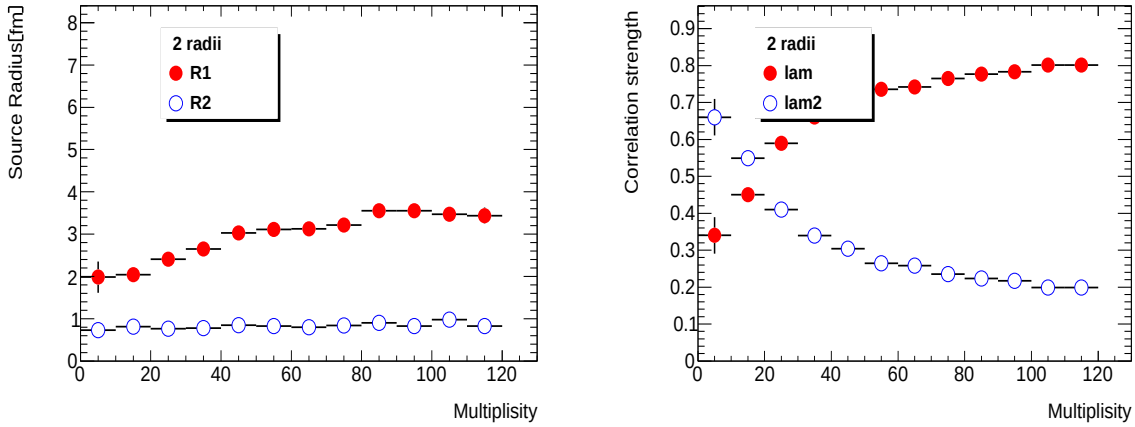

(a) Radiation source size as multiplicity

(b) Correlation strength

Figure 2: Fit results with two radii correlation functions for LHC beam energy 7 TeV with an integration over k_t

the 'Pomeron' denotes the subset of Feynman diagrams which provides the interaction across a large rapidity gap, and whose cross section does not decreases with energy. This may be BFKL pomeron built of gluons [10] or the multiperipheral ladder diagrams based on the colorless hadron degrees of freedom. It was studied first by Amati et al. in [11]. In the case of general purpose Monte Carlo (MC) generators such an elementary interaction is described by some hard subprocess supplemented by the backward DGLAP evolution down to the low scale proton wave function. Each time we deal with the colorless object which in general can be decomposed in terms of the colorless (hadron) degrees of freedom [5].

We have to emphasize that all the process of multi-particle production can be described in terms of the colorless objects – incoming colorless hadron wave function, new colorless pairs produced from the vacuum fluctuations and the secondary color dipoles (or more complicated but the colorless objects). That is it can be reworded in terms of the colorless (hadron) degrees of freedom. Indeed, many years ago V.N. Gribov discussed the possibility to treat the Pomeron as the high energy vacuum fluctuation which contains the $\ln s$ Feynman partons including the "wee" partons with low rapidities in the wave function of a fast hadron. See [13] where the space-time structure of the process was analysed in details.

However the one Pomeron exchange is only the beginning of the story. Starting from the one Pomeron amplitude the s-channel unitarity generates the sequence of the multi-Pomeron diagrams [14]. The simplest and the most important subset of such diagrams is given by the eikonal model. It corresponds to the expansion of the elastic amplitude (calculated at fixed impact parameter b)

$$A(b,s) = i(1 - e^{-\Omega(b,s)/2}) \tag{6}$$

[5] In MC this is actually done via the hadronization algorithm, implemented, for example, as the LUND string [12].

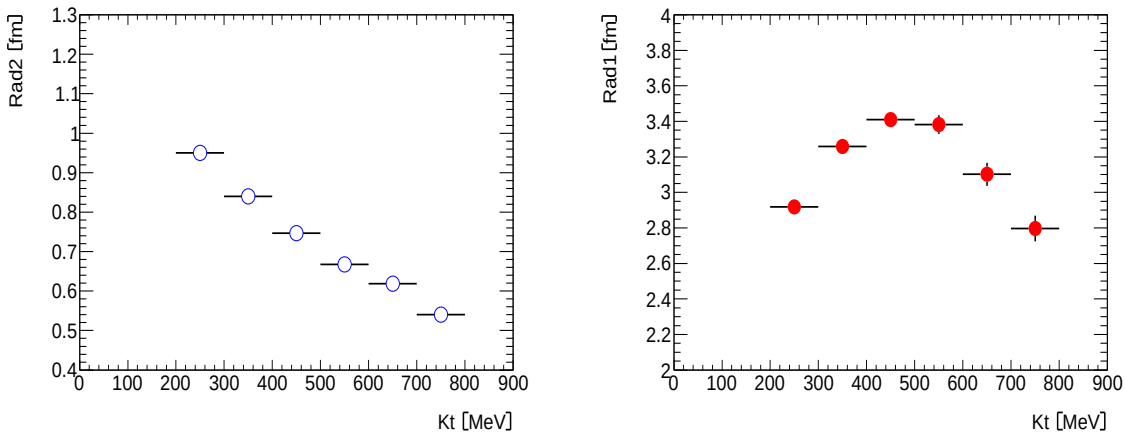

(a) R2 Kt dependence

(b) R1 Kt dependence

Figure 3: Fit results with two radii correlation functions for LHC beam energy 7 TeV with an integration over N_{ch}

in powers of opacity $\Omega(b,s)$. Then the multi-particle production from one or few 'cut' Pomerons can be calculated with the help of the AGK cutting rules [15].

Using the AGK rules it is easy to see that the mean number of 'cut' Pomerons $N_P = \Omega(b,s)$. In particular, for the central pp-collision at $\sqrt{s} = 7$ TeV based on the TOTEM elastic data [16] we expect $N_P = \Omega(0,s) \simeq 9$ [17]. Recall that according to AGK the particle density generated in the central rapidity interval is proportional to the number of cut Pomerons.

In the case of MC the process analogous to the multi-Pomeron exchange is generated via the Multiple Interaction (MI) option (see e.g. [18]).

That is in BEC we have to see at least two different radii - one corresponding to the correlation of two pions emitted from the same string/Pomeron and another one caused by the observation of two pions radiated from two different strings/Pomerons. The first radius is expected to be rather small. Its value is characterized by the value of the slope, α'_P of the Pomeron trajectory or by the typical scale in the DGLAP evolution chain generated by the MC. However, since it is 'measured' via the pion correlations (and a pion is not a point-like particle) it can not be much less than the pion radius $R^2_\pi \simeq 0.6\,fm^2$ fm.The second radius should be larger. The space separation between different Pomerons is of the order of two proton-proton interaction radius. The last can be evaluated through the total elastic slope B_{el}. The value of $B_{el} \simeq 20$ GeV^{-2} [16] corresponds to mean $R_p \sim 2.2$ fm [19].

The results presented in Fig.2,3 are in a good agreement with the picture described above. Indeed. The small radius R2 practically does not depend on the multiplicity, that is on the number of 'cut' Pomerons in an event (Fig.2a) and decreases with k_t. When with k_t increasing the resolution of our "femptoscop" improves we observe $R2 \rightarrow R_\pi$ (see Fig.3a). At a low multiplicities we deal mainly with the events caused by the one Pomeron exchange [6] and here the contribution of the small radius

[6] Of course distribution over the number of Pomerons is washed out due to the fluctuations in particle densities produced by the individual Pomerons.

component, $\lambda_2 = 1 - \lambda_1$, is large. At a larger N_{ch} which corresponds to a larger number of Pomerons, N_P, the value of λ_2 decreases while - λ_1 increases (see Fig.2b) since we have a larger combinatorial probability to observe two pions emitted from two different Pomerons. The value of large radius R1 increases with multiplicity – selecting the events with a larger N_{ch} i.e. - a larger N_P we consider the configurations with a larger area where the wave functions of two incoming protons overlaps. That is the Pomerons are distributed over a larger area. For a low k_t the value of R1 does not depends on k_t but for a larger k_t it starts to decrease (Fig.3b) – The events with a high transverse momenta (scales) are mainly concentrated in the central part of the collision area.

Note that the values of R1 observed at a large multiplicities are larger than that $2R_P$ evaluated from the elastic scattering slope $B_{el} = 20$ GeV^{-2}. This may be explained by the final state interaction/rescattering of secondaries in the case of a too large particle densities.

4 Conclusion

The experiment indicates that secondaries are produced by some small size sources distributed over a much larger (of order of the whole radiation size) domain. These sources may be considered as the individual Pomerons or as the minijets or the color strings between the jets which emit the 'spray' of hadrons.

The main result of the present paper is the following. We observe for the first time in BEC that the secondaries are produced by a number of *small* size sources (hot spots) of the radius $R2 \sim R_\pi$ (or smaller) with a much larger separation $R1 \sim 2R_p$ between the individual sources (hot spots). At last, not least, the value of the radius of a small size object is independent on LHC beam energy, i.e. this object is a universal one.

For a low particle density $dN_{ch}/d\eta < 2$ the radiation area is less than the proton size - that is we deal with only one hot spot.

In terms of the Quark-Gluon-Plasma/Liquid, that is in terms of collective degrees of freedom, our observation may be treated/interpretated as a hint in favour of scenario where the hadronization of quark-gluon system passes via the formation of a number of relatively small size colorless bubbles/drops which finally produce the hadrons.

Note however that due to a small size (R2) of radiative sources the probability of this "hot spots" to overlap is rather small even in the case of a heavy ions collision; while the energy density inside each small size "hot spot" is large.

4.1 Outlook

Having the particle identification it would be interesting to perform the two scales BEC fit for the kaons and/or the protons – are the space-time structure (BEC) of the production mechanism observed in this case is the same as that for the pions?

Next step is to study the two scales BEC in events with high E_T jet and/or W/Z bosons.

Finally, looking for the two scales BEC in the events with a Large Rapidity Gap (LRG) we expect to see a much smaller contribution of the large size component. Observing the LRG we select the events without an additional Pomeron exchange across the gap region. That is the probability of a Multiple Interaction is suppressed and in the first approximation one may say that the large size component should be absent. To be more precise we may observe some large size contribution corresponding to the multi-Pomeron exchange in the *Pomeron-proton* collision.

Acknowledgement

MGR was supported by the RSCF grant 14-22-00281.

References

[1] R. Hanbury-Brown and R.W. Twiss, Phil. Mag. **45**, 663 (1954); Proc. Roy. Soc. **242A**, 300 (1957); *ibid* **243A**, 291 (1957).

[2] G. Goldhaber, W.B. Fowler, S. Goldhaber et al., Phys. Rev. Lett. **3**, 181 (1959).

[3] G.I. Kopylov and M.I. Podgoretskii, Sov. J. Nucl. Phys. **15**, 219 (1972); **18** 336 (1973).

[4] G. Alexander, Rep. Prog. Phys. **66**, 481 (2003).

[5] ATLAS Collaboration, G. Aad et al., Eur. Phys. J. **C75** (2015) 466.

[6] CMS Collaboration, V. Khachatryan et al., JHEP **1105** (2011) 029.

[7] ALICE Collaboration, K. Aamodiet et al., Phys. Rev. **D84** (2011) 112004.

[8] V.A. Khoze, A.D. Martin, M.G. Ryskin and V.A. Schegelsky, Eur.Phys.J. **C76** (2016) 193

[9] UA1 Collaboration: C. Albajar et al., Phys. Lett. **B226**, 410 (1989).

[10] B. L. Ioffe, V. S. Fadin and L. N. Lipatov, "Quantum chromodynamics: Perturbative and non-perturbative aspects," (Cambridge, UK: Univ. Pr. (2014) 585 p).

[11] D. Amati, A. Stanghellini and S. Fubini, Nuovo Cim. **26**, 896 (1962).

[12] Bo Andersson, G. Gustafson, C. Peterson Z.Phys. C1 (1979) 105;
Bo Andersson, G. Gustafson, G. Ingelman, T. Sjostrand Phys.Rept. 97 (1983) 31-145.

[13] V.N.Gribov, The Theory of Complex Angular Momenta, Appendix A1, Cambridge University Press, 2003.

[14] V. N. Gribov, Sov. Phys. JETP **26** (1968) 414 [Zh. Eksp. Teor. Fiz. **53** (1967) 654].

[15] V. Abramovsky, V.N. Gribov and O.V. Kancheli, Sov. J. Nucl. Phys. **18** (1964) 308.

[16] G. Antchev *et al.* [TOTEM Collaboration], Europhys. Lett. **101**, 21002 (2013).

[17] M.G. Ryskin, A.D. Martin and V.A. Khoze, Eur.Phys.J. **C72** (2012) 1937

[18] T. Sjostrand, S. Mrenna and P. Z. Skands, Comput. Phys. Commun. **178**, 852 (2008) [arXiv:0710.3820 [hep-ph]].

[19] V.A. Schegelsky, A.D. Martin, M.G. Ryskin and V.A. Khoze, Phys.Lett. **B703** (2011) 288-291.